CSIRO PUBLISHING

Publications of the Astronomical Society of Australia, 2012, **29**, 1–11
http://dx.doi.org/10.1071/AS11003

A Model for Contact Binary EP Andromedae

Davood Manzoori

Department of Physics, University of Mohaghegh Ardabili, PO Box 179, Ardabil, Iran.
Email: d.manzoori@uma.ac.ir

Abstract: This paper presents the first comprehensive study of the EP And system, a contact binary. In this work the solution of the standard V light curve was obtained using the PHOEBE program (version 0.3c). Absolute parameters of the stellar components were then determined, enabling us to discuss the structure and evolutionary status of the close binary EP And. The times of minima data ('O−C curve') were analyzed. It was found that a third body with a period of 41.20 yr and mass 0.15 $M_{\odot}$ is orbiting around the system. Also a modulating period of an 11.72-yr cycle along with a relative period increase of $\frac{\Delta P}{P} = 1.79 \times 10^{-7}$ were obtained, which were attributed to the magnetic activity cycle and mass transfer with rate $\frac{\Delta m}{m} = 9.98 \times 10^{-8}\,\mathrm{yr}^{-1}$ between the components, respectively.

Keywords stars: binaries: eclipsing — stars: evolution — stars: individual (EP And)

Received 2011 February 3, accepted 2011 October 4, published online 2011 November 23

1 Introduction

A highly evolved close binary star in which both components fill their Roche lobes is called a contact binary. When both components have just filled the bounding equipotential surface and one or both components are in asynchronous rotation, they are sometimes described as forming a double contact binary. More often, both components exceed the equipotential surface and share a common convective envelope, which is called an over-contact binary. Further expansion would carry the envelope to the equipotential surface that contains the outer Lagrangian point (L_2), through which material would then be lost from the system.

Contact binaries are known to be quite common among variable stars; their spatial density is approximately $10^{-4}\,\mathrm{pc}^{-3}$ (see Gettel et al. 2006 and references therein). The problem of existence of contact binaries was considered by Kuiper (1941), assuming the synchronous rotation of two stars in a circular orbit. He showed that, for close binary systems, two stars cannot be in physical contact unless their common outer surface lies between the inner and outer critical surface of the Roche model. Kuiper concluded that two stars cannot be in stable contact unless they have a unit mass ratio (i.e. $M_1 = M_2$). Contact binaries in which both stars overflow their Roche lobes and form a common envelope of material are usually formed from nearly normal main sequence stars. Lucy (1968) treated the problem mathematically and proved that Kuiper's result is true only for the radiative common envelope, but not for a star with convective envelope. Shu et al. (1976) resolved the problem, using specific entropy s, proposed by Lucy, so that s converges to a single value in the common convective envelope of two stars (i.e. $s_1 = s_2 = s$), via introducing a contact discontinuity between the common envelopes and the interior of the Roche lobe of the cooler star. Lucy (1976) assumed that in a cool contact binary, where both components are located on the zero-age main sequence (ZAMS), they evolve via thermal relaxation oscillation with a circular mass transfer from the secondary to primary component until the primary reaches a limiting mass for the CNO cycle to dominate the hydrogen burning process. The primary evolves then off the ZAMS and increases its radius so that both components can fill their critical Roche lobes being in thermal equilibrium. Hilditch (1989) confirmed Lucy's conclusions. Maceroni and Van't Veer (1996), revising the properties of numerous samples of W UMa stars, concluded that little correlation existed between the standard classification's A and W subtypes, which had earlier been proposed by Binnendijk (1970) on the basis of light-curve morphology. Furthermore, A-type contact systems could be considered as later evolutionary stages of W subtypes, and they suggested the A subtype could be divided into three different samples.

According to Stepien (1995; 2006) W UMa stars are magnetically very active and it is generally accepted that they lose mass and angular momentum (AM) via magnetized wind. Gazeas and Stepien (2008), analyzing over a hundred cool contact binaries, found several correlations among the geometrical and physical parameters and stated that 'the coalescence of both components into a single fast rotating star is the final fate of contact binaries'. This statement is not in agreement with that of Li et al. (2005). In a series of three papers, Li et al. (2004a; 2004b; 2005) discuss the structure and evolution of low-mass contact binaries, with and without spin and orbital angular momentum loss (AML), and taking into account effects of energy transfer, with negligible gravitational

radiation. They present an ultimate model of W UMa systems exhibiting cyclic evolution around a state of marginal contact, on timescales of about 6×10^6 yr without loss of contact, if spin angular momenta of both components are included; and about 9×10^6 yr, if spin angular momenta of both components are neglected. According to them, the ratio of the spin angular momenta of both components to the orbital angular momentum of the system becomes larger as the evolution proceeds, so that the system will coalesce into a rapidly rotating star when the spin angular momenta of both components become more than one third of the orbital angular momentum of the system. Recently Tylenda et al. (2011) have reported the merging of contact binary V 1309 Sco to a single object observationally. Hence the cyclic evolution mentioned for the contact binary systems cannot last forever. It only lasts about 7×10^9 yr, in good agreement with the observational result of the old cluster NGC188 (Kaluzny & Shara 1987), containing at least four W UMa–type stars. On the basis of Li et al.'s findings, Song et al. (2007) presented a model for contact binaries, in which they considered several features of this kind of star: energy, mass, AM exchange, and rotation.

To explain formations of binary stars, particularly contact binaries with higher-order multiplicity, Tokovinin et al. (2006) examined 165 solar-type spectroscopic binaries (SBs) with periods of 1–30 days. They found that, in contrast to their identical mass distribution, the period distributions in the systems with and without a tertiary component (TC) are quite different. They found that the frequency of occurence of a tertiary component is a strong function of SB period. They showed that frequency reaches 96% for $P < 3d$, and decreases to 34% for $P > 12d$; moreover, the periods of TCs range from 2 yr to 10^5 yr. Pribulla and Rucinski (2006) collected the available evidence for multiplicity of contact binaries with $V < 10$ mag: of 151 objects inspected, 64 were triple systems, hence they concluded that most contact binary stars do exist in multiple systems. D'Angelo et al. (2006) analyzed 4000 spectra from 75 close binaries for spectroscopic signature of tertiaries and identified 23 triple systems (almost one third). Rucinski et al. (2007) presented the results of a search for TC of a group of contact binaries and concluded that the presence of a close component is a very common phenomenon for very close binaries with orbital period < 1 day.

In this paper we will discuss the contact binary EP And with the following particulars: EP And = BV 75 (GSC 02827-00017, $V_{\max} = 11.45$ mag, spectral type F8 V). It was discovered by Strohmeier et al. (1955); the eclipsing nature of the system was first found by Filatov (1960); Manek (1994) describes a brief history of the system's discovery; the system was classified as a contact binary star by Gettel et al. (2006). The first photometric BV-light curves (LC) of the system seem to have been published by Pribulla et al. (2001), who determined (without giving the errors) only a few elements (i.e. q, the mass ratio; i, inclination of the orbital plane; and T_1, T_2, the effective temperatures of primary and secondary stars. They found that the secondary component is slightly hotter and the system is probably of W UMa type. Qian and Yuan (2001) studied the period of the system and reported a period increase with rate $dP/dt = 1.16 \times 10^{-7}$ d/yr, without pointing out the factors affecting the period change.

The present work utilizes the PHOEBE (PHysics of Eclipsing BinariEs code, version 0.3c (Prsa and Zwitter 2005; Prsa et al. 2008), which is a photometric program based on the Wilson–Devinney code (see Wilson and Devinney 1971, Van Hamme and Wilson 2003) and produces corresponding parameters, as well as absolute dimensions, from which we can discuss the evolution of the system. We also analyze O−C data and discuss variations of the orbital period.

2 Light-Curve Modeling and Spot Analysis

The photometric data were selected in the Johnson V-passband filter from the website of the American Association of Variable Stars Observers (AAVSO). These data were obtained on 26 and 29 October and 25 November 2007. The stars HD 70123 and HD 71024 were used as comparison and check, respectively, and the following ephemeris was used to convert all the data to a phase–magnitude system, given by the fourth edition of the General Catalogue of Variable Stars (Kolopov et al. 1985):

$$T_{\min \mathrm{I}} = 2442638.5109 + 0.40411057\mathrm{E}. \qquad (1)$$

In addition to the above-mentioned data, photometric data of this system from the Super WASP (Wide Angle Search for Planets) project, collected in the years 2006–2008 in a broadband filter with a passband from 400 to 700 nm (for details see Butters et al. 2010), were also analyzed (by the method described below). The results of this last dataset LC solution are summarized in Table 1 (column 3) and observed and synthetic LCs are displayed in Figure 1. Figure 2 displays residuals between the synthetic and observed LCs.

The times of minima listed in Table 2 were determined from AAVSO data using the method of Kwee and Van Woerden (1956). PHOEBE version 0.3c was used to obtain the solution of the LC. Since no spectroscopic data were available, a q search was performed in order to obtain an initial value for the mass ratio. This search, which consists of running the program keeping q constant for a set of q values > 0.3 (e.g., 0.31, 0.32 and so on) and choosing the minimum residuals as initial value (see Figure 3). The best case (for q range) was between 0.35 and 0.40. The gravity-darkening coefficients $g_1 = g_2 = 0.32$ and bolometric albedos $A_1 = A_2 = 0.50$ were assigned theoretical values corresponding to a convective envelope. The values of limb-darkening coefficients were automatically interpolated step by step with PHOEBE according to the limb-darkening tables of Van Hamme (1993) for a relative abundance [M/H] = 0.1 (see Wilson & Van Hamme 2003). The other parameters, i.e., q, the mass

https://doi.org/10.1071/AS11003 Published online by Cambridge University Press

Table 1. The results obtained through light-curve analysis using PHOEBE

Parameter	Values for AAVSO LC	Values for WASP LC
i (°)	81.45 ± 0.05	81.50 ± 0.04
T_1 (K)	6400 ± 153	6280 ± 189
T_2 (K)	6280 ± 151	6150 ± 183
$\Omega_1 = \Omega_2$	2.626 ± 0.003	2.628 ± 0.004
q	$0.395 \pm .001$	$0.394 \pm .001$
$(\frac{L_1}{L_1+L_2})V$	0.712 ± 0.010	0.712 ± 0.02
$(\frac{L_2}{L_1+L_2})V$	0.288	0.288
r_1(pole)	0.442	0.441
r_1(side)	0.473	0.473
r_1(back)	0.503	0.502
r_2(pole)	0.290	0.289
r_2(side)	0.303	0.302
r_2(back)	0.342	0.340
Fillout	17.4%	15.7%
$X_{1,V} = X_{2,V}$	0.53	0.54
$A_1 = A_2$	0.50	0.50
$g_1 = g_2$	0.32	0.32
Spot parameters		
Colat (°)	47.00	55.00
Long (°)	180.00	190.00
Size (°)	20.00	20.00
Temp factor	0.95	0.90
	$\chi^2 = 0.025$	$\chi^2 = 1.830$

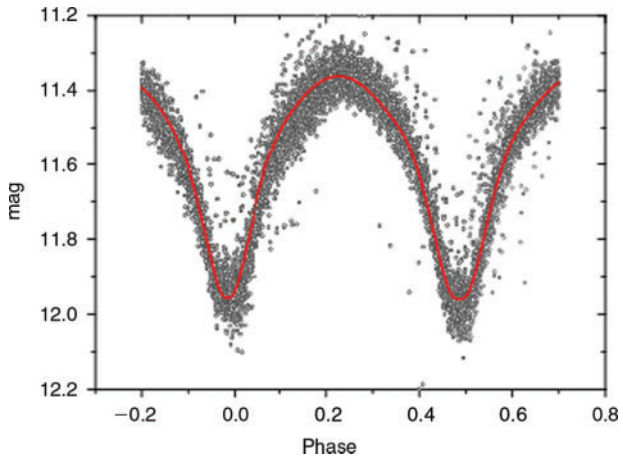

Figure 1 Synthetic light curve (continuous curve) obtained using over-contact mode of PHOEBE, and observed light curve (filled circles) of Super WASP data, fitted based on the calculated parameters in Table 1 and spot parameters of Table 1 for EP And.

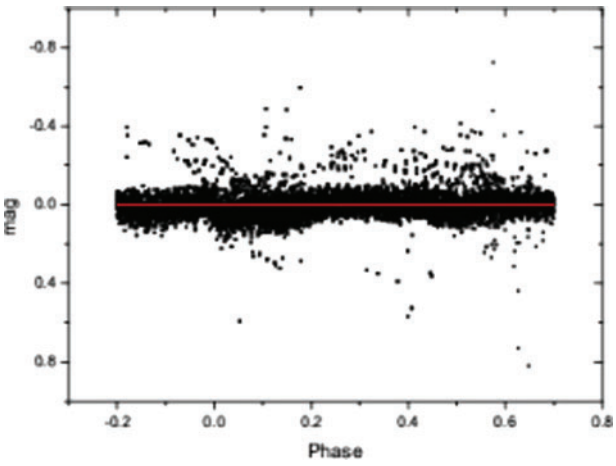

Figure 2 Residuals between the synthetic and the observed light curve for Super WASP data.

Table 2. Times of minima obtained through observations in V passbands

Min I (HJD)	Min II (HJD)
$2454399.7344380 \pm 0.000084$	$2454402.765150 \pm 0.000152$
$2454429.637761 \pm 0.000147$	$2454429.840451 \pm 0.000117$
$2454402.967609 \pm 0.000249$	

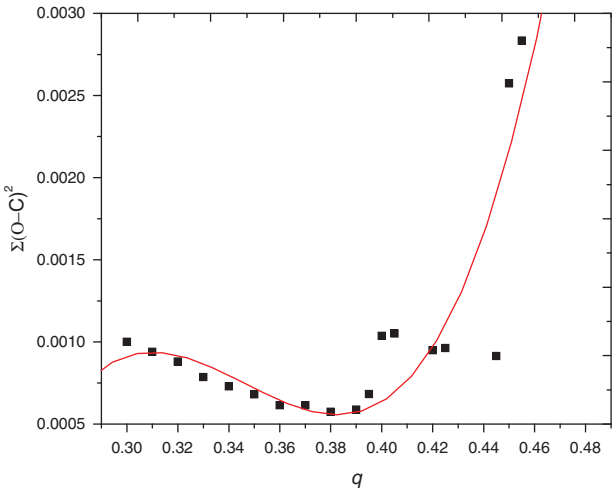

Figure 3 The relation between q and Σ for EP And.

ratio; Ω_1, the modified Kopal potential of the primary; i, the orbital inclination; T_1, T_2, temperatures of the primary and secondary components respectively; and L_1, the luminosity of the primary component, were set as free. The free parameters were adjusted sequentially by trial and error. The calculated parameters are listed in Table 1 (column 2). While the normal points and synthetic LCs are illustrated in Figure 4. Figure 5 illustrates the residuals between the observed data and synthetic LC. All the parameters with subscript '$\odot$' refer to the relevant quantities of the Sun. The errors of parameters listed in Table 1 are mean statistical errors. It was observed that (for both sets of data) the synthetic LC could be best fitted to the observed data points by assuming a rather large dark spot on the primary, the details of which were added to Table 1. The positions of the spot on the component star along with the Roche geometry of the system (for AAVSO data) were as denoted in Figure 6.

3 Absolute Dimensions

Since no spectroscopic data is available for this system, the absolute dimensions of EP And may be estimated via the $B - V$-based absolute magnitude–color relation of Rucinski & Duerbeck (1997), i.e. $M_V = M_V(\log P, B - V)$.

https://doi.org/10.1071/AS11003 Published online by Cambridge University Press

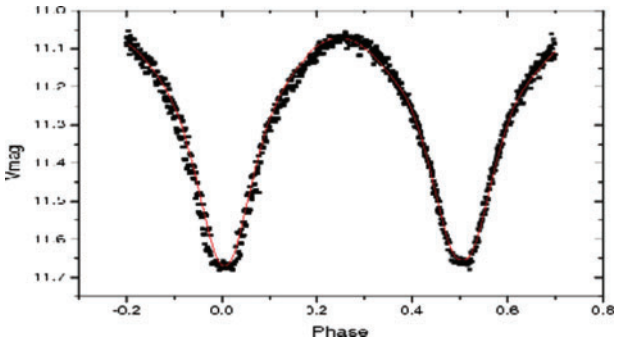

Figure 4 Synthetic light curve (continuous curve) obtained using over-contact mode of PHOEBE, and observed light curve (filled squares) in V filter, fitted based on the calculated parameters in Table 1 and spot parameters of Table 1 for EP And.

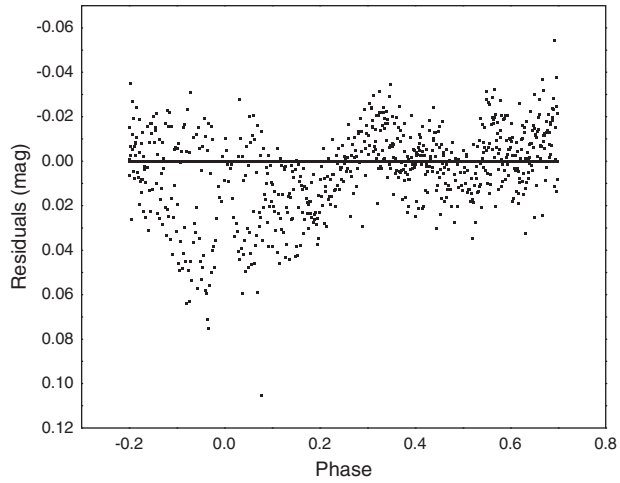

Figure 5 Residuals between the synthetic and the observed light curve in V filter.

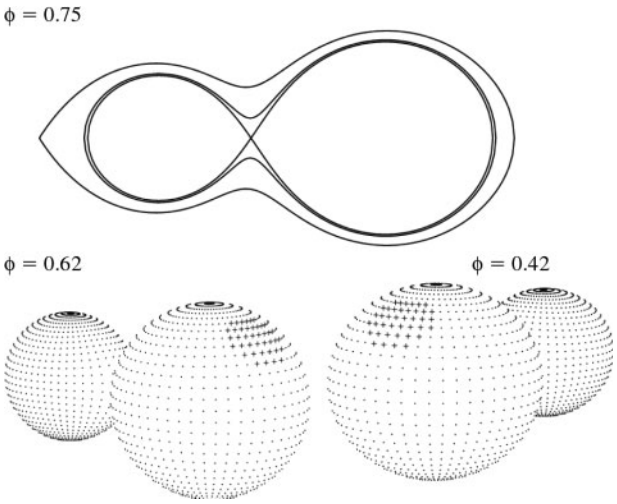

Figure 6 Representation of spotted region (darker area) on the surface of the primary and Roche surfaces of EP And.

This period-luminosity-color calibration has the following form:

$$M_v = -4.42 \log P + 3.08(B-V) + 0.1 \qquad (2)$$

Table 3. Absolute physical and orbital parameters of the EP And system, obtained through LC analysis

Parameter	Values for AAVSO LC	Values for WASP LC
M_V	3.96 ± 0.64	
Period	0.404111 ± 0.0000011(adopted)	
$a\ (R_\odot)$	2.49 ± 0.38	
$M_1/M_\odot$	0.94 ± 0.09	0.91 ± 0.13
$M_2/M_\odot$	0.38 ± 0.05	0.36 ± 0.05
$R_1/R_\odot$	1.18 ± 0.05	1.17 ± 0.25
$R_2/R_\odot$	0.77 ± 0.03	0.76 ± 0.16
$L_1/L_\odot$	2.21 ± 0.01	2.10 ± 0.02
$L_2/L_\odot$	0.89	0.59
$M_{1,\mathrm{bol}}$	4.18 ± 0.52	4.04 ± 0.90
$M_{2,\mathrm{bol}}$	3.54 ± 0.70	4.98 ± 0.96
$B-V$	0.62 ± 0.21 (Pribulla et al. 2001)	

where the value $B-V = 0.626 \pm 0.209$ mag has been taken from Pribulla et al. (2001). Hence $M_v = 3.96 \pm 0.60$ and interstellar extinction $A_v = 0.16$. Accepting that $m_v = 11.10$, the distance of the system was estimated as $d = 250 \pm 32$ parsec. From the absolute and visual magnitudes the bolometric luminosities can be computed (we used Flower's 1996 table to determine the bolometric corrections from the temperatures). By using the relations

$$\frac{L_{1,2}}{L_\odot} = \left[\frac{R_{1,2}}{R_\odot}\right]^2 \left[\frac{T_{1,2}}{T_\odot}\right]^4 \qquad (3)$$

$$R_{1,2} = a r_{1,2} \qquad (4)$$

$$\frac{a}{R_\odot} = [IP^2(m_1+m_2)]^{1/3} \qquad (5)$$

$$M_{\mathrm{bol},1,2} = 42.36 - \log T_{1,2} - 5\log(R_{1,2}/R_\odot) \qquad (6)$$

and values listed in Table 1, estimates were made of a, the orbital separation; m_1, m_2 masses; R_1, R_2 radii of the individual components; and M_{bol}, the bolometric magnitude. The results are tabulated in Table 3. Equation 3 above can easily be derived from Stefan's law of radiation, which is a relation between the flux emitted by a star and the fourth power of surface temperature. By treating m_1, m_2 (in solar units) and I as constants, Equation 5 is simply the mathematical statement of Kepler's third law, which relates the square of orbital period P (in days) to the third power of the orbital radius a (in solar radii). Equation 6 is an empirical relation between the bolometric magnitude and logarithmic temperature and radius of the stars (see Wesselink 1969).

4 O−C Curve Analysis

The O−C data points were collected from different sources,[1] mainly from (the updated) website of the Czech Astronomical Society, O−C webpage, to which five

[1] i.e., the websites of the AAVSO (`http://www.aavso.org`) and Cracow Eclipsing Binaries Minima Database (`http://www.as.up.Krakow.pl/o-c/`)

https://doi.org/10.1071/AS11003 Published online by Cambridge University Press

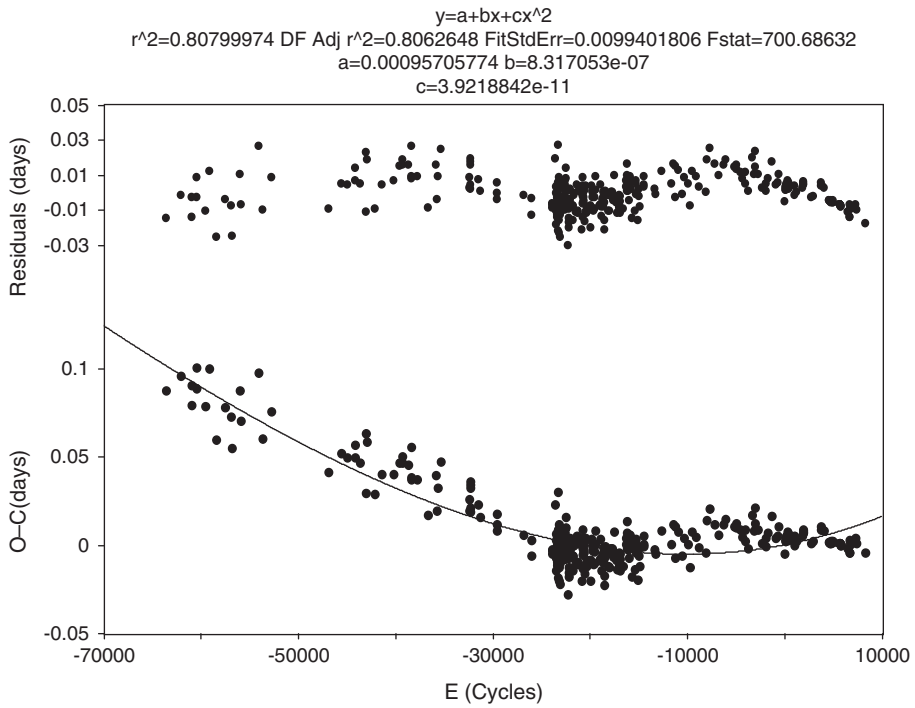

Figure 7 The lower plot indicates O−C residual values (filled circles) and their description by an upward-curved semi-parabola (continuous curve). The upper plot represents the residuals between the fitted parabola and observed O−C points for EP And.

times of minima reported in Table 2 of the present work were added. Then, using the following ephemeris

$$T_{\min \mathrm{I}} = 2452137.525 + 0.40411E \qquad (7)$$

these data were converted to a common epoch, then all the O−C values (including $(O–C)_1$ and $(O−C)_2$, the primary and secondary residuals, respectively) were plotted against E (Epoch cycles) in Figure 7. For the calculations of $(O−C)_2$ residuals, a term $\frac{E}{2}(0.40411)$ was added to the above Equation 7.

The general trend of O−C values displayed in Figure 7 may be roughly fitted by an upward-curved semi-parabola, the coefficients of which, along with correlation coefficients and statistical errors, are given just above Figure 7. Also the residuals between the fitted parabola and O−C normal points are displayed in the upper portion of the Figure 7. Since the general trend of residues indicate a wavelike character, to carry on further analysis we plot them separately in Figure 8. They are best fitted by a Fourier series polynomial, the coefficients of which are given just above the figure and the residuals are displayed in the upper portion of the same figure. The wavy character of Figure 8 indicates some alternating phenomena modulating the orbit period (see Manzoori 2007) of the EP And system. The analysis of this curve gives a period of $P_3 \simeq 41.20$ yr, which may be attributed to the presence of a third body orbiting the system with semi-major axis $a_3 \sim 22.00 \pm 2.98 R_\odot$. The lower limit to the mass (m_3) of this third body (for $i_3 = 90°$) may be estimated from the well-known equation of mass

$$F(m) = \frac{(a \sin i)^3}{P_3^2} = \frac{(m_3 \sin i_3)^3}{(m_1+m_2+m_3)^2} \qquad (8)$$

as $m_3 = 0.15 \pm 0.01 \mathrm{M}_\odot$, where a = orbital radius of the binary around the common barycenter of mass; $m_1 = 0.94 M_\odot$, the mass of the hot component (primary); and $m_2 = 0.38 M_\odot$, the mass of the cool component (secondary), were taken from Table 3.

To reveal any further cyclic behavior, the Fourier polynomial is subjected to Fourier decomposition, the frequency spectrum of which is displayed in Figure 9. As is evident from Figure 9, there is a distinct peak well above the noise level in the Fourier spectrum at a frequency of 9.43×10^{-5}cycle^{-1} corresponding to a period of 11.72 yr. This may be attributed to a magnetic activity cycle effect operating in the system. For further interpretation and discussion, see Section 6.5.

Apart from the period 11.72 yr, there is another notable peak at frequency 0.00162 cycle^{-1} corresponding to a period of 0.64 yr, which seems to be due to windows in (unevenly sampled) data and therefore has no physical significance.

5 Mass Transfer

As stated in Section 4, the overall trend of the O−C data points, plotted in Figure 7, can be approximated by a rough upward-curved parabola (the continuous curve) which indicates a secular increase in the period with a rate $\mathrm{d}P/\mathrm{d}E = 7.84 \times 10^{-11}$ d/cycle (or $\mathrm{d}P/\mathrm{d}t = 6.12 \times 10^{-3}$ sec/yr) estimated in this work. This overall secular variation may be attributed to mass ejection in the system.

Now it is a well-known fact that normally, in contact binaries, both components have filled their Roche lobes and have a common envelope; moreover, due to their low separation distance, a strong mutual gravitional force exists between them so that it can accrete matter from

https://doi.org/10.1071/AS11003 Published online by Cambridge University Press

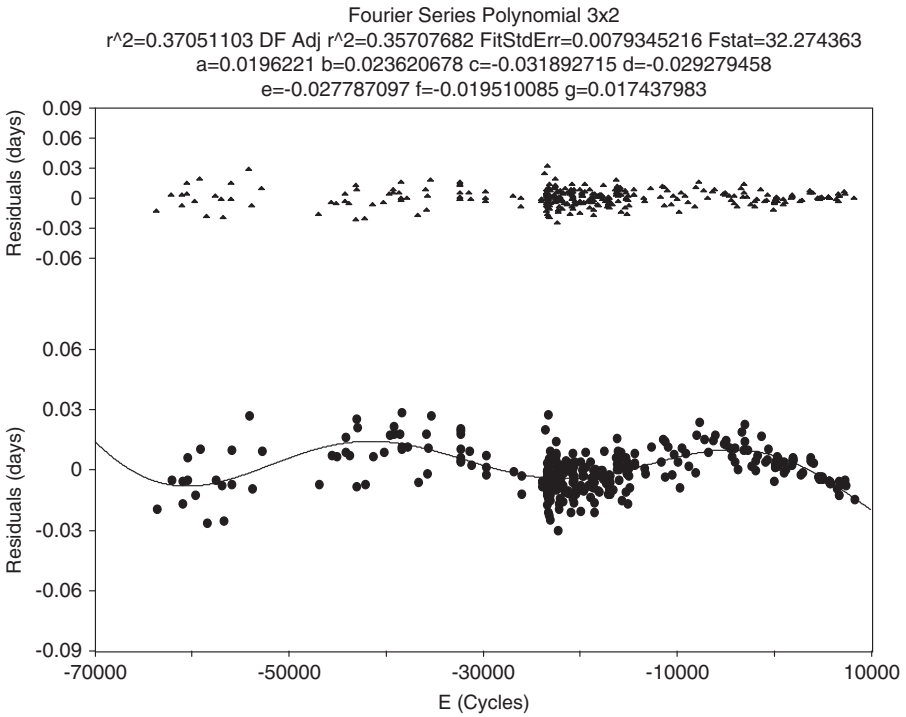

Figure 8 The lower plot indicates the fitted polynomial (continuous curve) to the residuals between the observed O−C differences and the fitted parabola. The upper plot represents the differences between the fitted polynomial and the residual points for EP And.

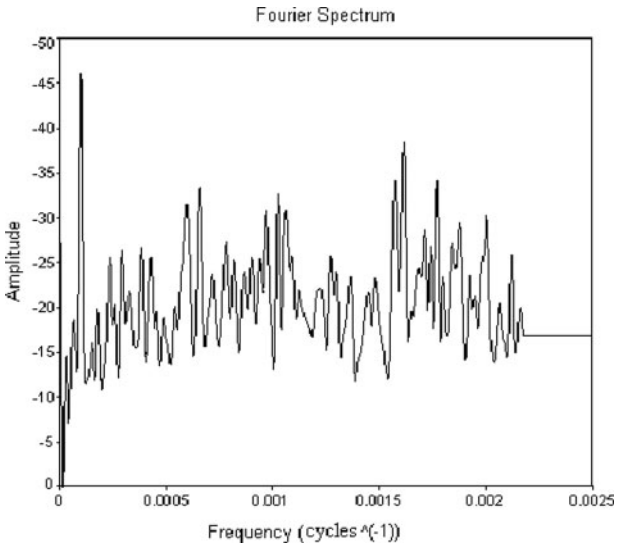

Figure 9 The Fourier (frequency) spectrum of the Fourier polynomial fitted to O−C residual values of EP And. The periodogram was created after removing the 41.2-yr period.

the surface of the other component star and exchange of mass will take place between the components. In addition, some loss of mass and angular momentum may occur from the outer Lagrangian point which may affect the orbital period significantly. Figure 6 illustrates the Roche surface of the system, obtained using the V passband filter data from Table 1. As is obvious from the figure, both of the components have completely filled their Roche lobes and are therefore capable of transferring mass and forming a common envelope. Assumption of conservative mass flow is the most likely process of mass transfer in this system due to a rather low distance between the two components. Hence, assuming a conservative case (i.e., where no matter leaves the system) and using the relative period rate of change $\Delta P/P = 1.79 \times 10^{-7}$ obtained in this work and the equation

$$\Delta m_2/m_2 = -\frac{m_1}{3(m_1 - m_2)}\frac{\Delta P}{P} \tag{9}$$

from Huang (1963), a relative mass transfer of $\Delta m_2/m_2 = 9.98 \times 10^{-8}\,\mathrm{yr}^{-1}$ and hence the corresponding mass and angular momentum lost by the secondary were obtained as $\Delta m_2 = -3.69 \times 10^{-8}\ m_\odot\,\mathrm{yr}^{-1}$ and $\Delta J = -2.54 \times 10^{46}\,\mathrm{g\,cm^2\,s^{-1}}$, respectively; where the masses of the components m_1 and m_2 have been used from Table 3 (column 2)[2] and Equation 10 below from Applegate (1992).

Transfer of mass and *cyclic magnetic activity* (see Sections 6.3 and 6.5) in binary stars containing at least one late-type star would cause the orbital parameters like J (orbital angular momentum), a (orbital radius) and ω (angular speed) to change accordingly. Here we follow Applegate (1992), Kalimeris et al. (1994) and Lanza et al. (1998) to estimate some of these quantities for a conservative case as below:

$$\Delta J = -\frac{Gm_2^2}{R}\left(\frac{a}{R}\right)^2\frac{\Delta P}{6\pi} \tag{10}$$

$$\Delta E' = \omega_{dr}\Delta J + \frac{(\Delta J)^2}{2I_{\mathrm{eff}}} \tag{11}$$

[2]In the following estimations of the system parameters, only the values of column 2 from Table 3 are used, due to their greater accuracy.

https://doi.org/10.1071/AS11003 Published online by Cambridge University Press

Table 4. The estimated parameters corresponding to modulation period 11.72 yr

Parameter	Secondary	Primary
$\frac{dP}{dt}$ (s yr^{-1})	6.12×10^{-3}	6.12×10^{-3}
ΔJ (g cm^2 s^{-1})	-2.54×10^{46}	-4.72×10^{46}
$\Delta E'$ (erg)	4.49×10^{39}	8.10×10^{39}
$\Delta L_{\rm rms}$ (erg s^{-1})	-3.81×10^{31}	-6.88×10^{31}
$\frac{\Delta\omega}{\omega}$	0.001	0.0006
ΔQ (kg m^2)	4.01×10^{40}	1.01×10^{41}
B (kG)	92.10	67.80
$\frac{da}{dE}$ (cm cycle^{-1})	7.98×10^{-11} [2.465e20]$^{0.33}$	
ω (rad s^{-1})	5.62×10^{-4}	5.72×10^{-4}
$\frac{d\omega}{dE}$ (rad cycle^{-1})	3.10×10^{-9}	3.11×10^{-9}

$$\Delta L_{\rm rms} = \pi \frac{\Delta E}{P_{\rm mod}} \tag{12}$$

$$\frac{\Delta\omega}{\omega} = \frac{GM^2}{3R^3 M_s}\left(\frac{a}{R}\right)^2\left(\frac{P}{2\pi}\right)^2\frac{\Delta P}{P} \tag{13}$$

$$\Delta Q = -\frac{MR^2}{9}\left(\frac{a}{R}\right)^2\frac{\Delta P}{P} \tag{14}$$

$$N \sim \frac{B^2}{4\pi}(4\pi R^2)\Delta R \sim 0.1 B^2 R^3 \tag{15}$$

$$B^2 \approx 10\frac{GM^2}{R^4}\left(\frac{a}{R}\right)^2\frac{\Delta P}{P_{\rm mod}} \tag{16}$$

$$\frac{da}{dE} = \left[\frac{2G(m_1+m_2)}{27\pi^2}\left(\frac{1}{P}\right)\right]^{\frac{1}{3}}\frac{dP}{dE} \tag{17}$$

$$\frac{d\omega}{dE} = \frac{2\pi}{P^2}\frac{dP}{dE} \tag{18}$$

where $a/R = 3.23$, in which R is the radius of the secondary component, $\Delta P = 0.073$ s, the orbital period change during the 11.72-yr cycle, and $\Delta E'$ is the energy required to transfer angular momentum ΔJ. M and M_s are masses of the component stars and surrounding shell, I_s and I_* are moments of inertia of the surrounding shell and star, respectively, so that $I_s \approx I_* \approx 2I_{\rm eff}$, and $I_{\rm eff} = I_s\, I_*/(I_s + I_*)$, ΔQ is the gravitational quadrupole moment of the active star, **B** is the subsurface magnetic induction field, da/dE and $d\omega/dE$ are the rates of change of orbital radius and orbital speed, respectively. Using Equations 10–18, and modulating period $P_{\rm mod} = 11.72$ yr, we obtained the quantities listed in Table 4. Apart from **B**, the magnetic induction field, which shows comparatively high values (see Section 6.5 for interpretation), the values estimated (in Table 4) are fairly well in agreement with the corresponding values estimated by Applegate (1992) for the other systems.

To compare the results of Applegate and Lanza, we used Equations 19 and 20 below, borrowed from Lanza (1998),

$$\Delta Q = \frac{-Ma^2}{9}\frac{\Delta P}{P} \tag{19}$$

$$\frac{\Delta\omega}{\omega} = \frac{9}{8K_2}\frac{G}{R^5\Omega^2}\Delta Q \tag{20}$$

to estimate the values of $\Delta Q = 3.95 \times 10^{39}$ kg m^2 and $\Delta\omega/\omega = 1.55 \times 10^{-3}$, where K_2 is the apsidal motion constant; these values were found to be in rough agreement with the corresponding values calculated from Equations 13 and 14 above. Also by comparison of ΔQ with the values given by table 1 of Lanza (2005) and table 2 of Lanza (2006), one finds fair agreement between these values.

6 Conclusions and Discussion

6.1 Light Curve

By considering the shape of the observed LCs, and since the EP And system was defined as a probable W UMa type star by Pribulla et al. (2001), the attempt was made to obtain LC solutions (and best fit to the observed data) in the over-contact W UMa mode of the PHOEBE program. The LC solutions (described in Section 2) indicate that EP And is a shallow-contact binary, i.e. fillout $f = \frac{\Omega_{in}-\Omega}{\Omega_{in}-\Omega_{out}} = 16.6\%$.

It seems that this system is a marginal-contact binary, and the flat bottom of the secondary eclipse confirms an A-type W UMa subclass. The LC does not seem to display significant night-to-night variations, except at out-of-eclipse phases. The vertical offset at out-of-eclipse phases might be due to star spots, a small O'Connell effect (≈ 0.02 magnitude) on the system cannot be ignored. The mass ratio $q = 0.395 \pm 0.001$ obtained in this work differs from that of Pribulla et al. (2001), which was 0.340. Despite the marginal contact, the temperature difference between the components (i.e. $\Delta T = 120$ K) is not high. This means that the spectral type of the components is close to each other. The behavior of the orbital period is in good agreement with the magnetically driven angular momentum loss (AML) hypothesis (Van't Veer & Maceroni 1989). This theory predicts that in the contact phase the magnetic torque can cause contact binaries to evolve to extremely low mass ratios which suggests a mass transfer from the secondary to more massive primary and consequently we have to observe period increase (in fair agreement with the results reported in Sections 5 and 6.3 of this paper). Most of the authors (if not all) believe that all the W UMa type binary stars may contain cyclic period variations.

6.2 Evolutionary Status

In the Figures 10–12 we have illustrated the evolutionary status of EP And on the Mass-Luminosity, Mass-Radius and H-R diagrams, adopting the values given in Table 3. To draw these diagrams, we have computed the related stellar parameters of theoretical ZAMS for metallicity $Z = 0.1$, using the theoretical isochrones calculator of Siess et al. (2000, & `http://www-astro.ulb.-ac.be/siess/server/iso`). Then the obtained values along with the respective quantities of EP And are depicted in Figures 10–12. All the three diagrams indicate that the secondary is a little more evolved along the Main Sequence than the primary, but the primary is

https://doi.org/10.1071/AS11003 Published online by Cambridge University Press

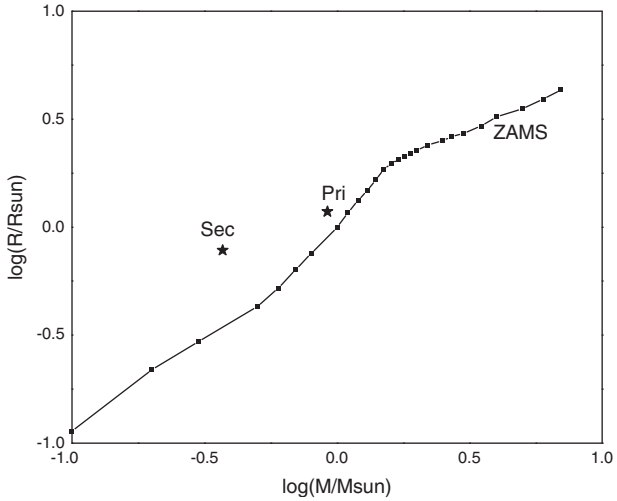

Figure 10 Mass–radius diagram and positions of both components of EP And.

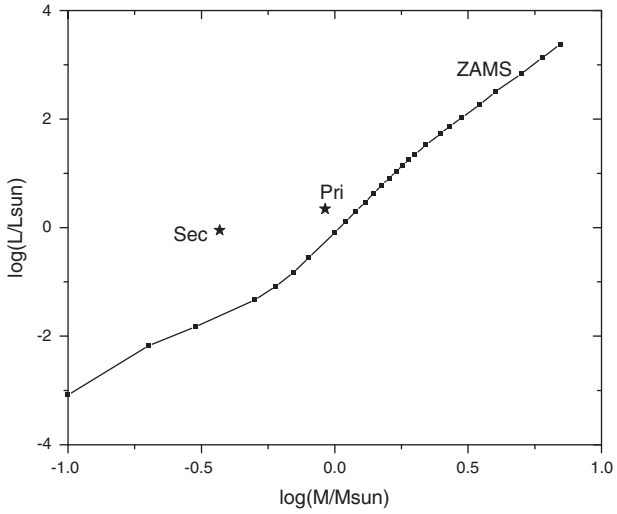

Figure 11 Mass–luminosity diagram and positions of both components of EP And.

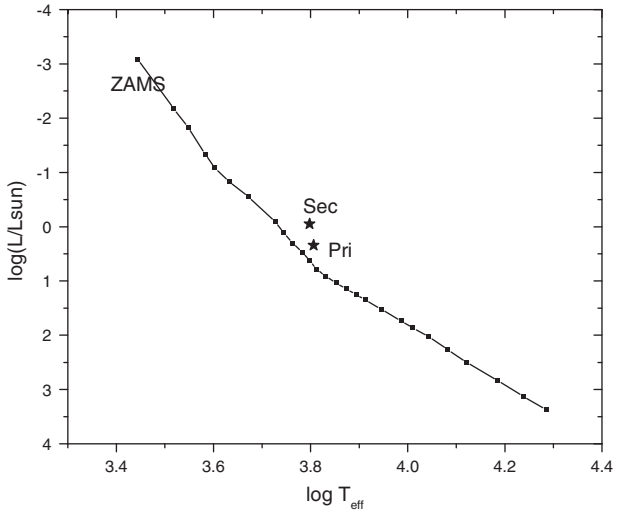

Figure 12 H–R diagram and positions of both components of EP And.

comparatively less evolved, i.e. it is a Main Sequence (or nearly Main Sequence) star consistent with the theories (see Lucy 1976). To study the structure of the system in more detail the spectroscopic data is required.

6.3 Orbital Period Variations

Orbital period study in this type of systems is very useful to understand their structure and evolution. It can provide estimates of mass and AML which are predicted by some theoretical works (see Section 5 and Table 4 for the corresponding estimated values of EP And). The O−C diagrams formed by the minimal times of eclipses provide the basis for studying time-dependent period variations of eclipsing binaries.

As stated earlier in Section 4, one of the main characteristics of contact (W UMa type) binaries is mass transfer due to Roche lobe filling of the components, such mass exchange will spin up the mass accreting star (most of whose mass is transferred material by the end of rapid phase of mass transfer). However according to Wilson et al. (1985) this rapid rotation will be damped quickly, as soon as the mass transfer is stopped. Thus, near to or after the end of rapid phase of mass transfer, the mass losing star would normally be found to fill its Roche lobe (rotating synchronously), while the accreting star (or perhaps only its outer envelope) may have accommodated all of its capacity of the angular momentum which can hold, and so fill its limiting 'rotational' lobe, thus forming a double contact asynchronous system.

Visual inspections of the O−C data points plotted in Figure 5 reveal that the general trend of plotted points in Figure 5 can be approximated by a rough upward semi-parabola (i.e., the continuous curve), which indicates a secular increase in the period with the rate $\mathrm{d}P/\mathrm{d}t = 6.12 \times 10^{-3}$ sec/yr, estimated in this work. This secular period increase can be explained in terms of mass transfer from the less massive to the more massive hotter star with the rate of $-3.69\times10^{-8}\ m_{\odot}$/yr. According to Biermann & Hall (1973), the dynamical instabilities initiate a sudden transfer of mass from cooler star and decrease the period, as angular momentum is temporarily stored as faster than synchronous rotation in or around the hotter star. Then the angular momentum is returned to the orbit on a friction time scale and the period increases.

6.4 The Third Body

As pointed out in the first section, most of the contact binaries particularly those having orbital period $<3d$ are found in multiple systems. Moreover the wavy character of the residuals between the observed O–C data and fitted parabola (as mentioned in Section 4), might be attributed to the presence of a third body circling the system with a period of 41.2 yr and mass $0.15 \pm 0.01 M_{\odot}$.

As pointed out in Section 3, this system has not been observed spectroscopically, due to faintness. Apart from adaptive optics methods, D'Angelo et al. (2006) suggested three methods for improving the observations of

https://doi.org/10.1071/AS11003 Published online by Cambridge University Press

low mass and faint tertiaries such as EP And system, as follows:

1 – By use of Echelle spectrograph with high resolution and wide range of wavelengths. 2 – Observations at longer wavelength. 3 – Coverage of a large fraction of tertiary parameters. We encourage the spectroscopic observations of this system by taking into account the suggestions of D'Angelo et al. (2006).

6.5 Magnetic Cycle Effect

Referring to Section 4 and Figure 9, the Fourier analysis of the polynomial fitted to the residual values between O−C data and parabolic fit gave a period of 11.72 yr cycle modulating the orbital period. This may be attributed to the magnetic activity cycle operating in this system. A result which is well agreed with Galownia (2002) results of O−C analysis for a large sample of W UMa-type stars that 'every system changes period, the mean interval of period stability is about 11 yr and most promising explanation of these changes seems to be magnetic activity for all W UMa systems'. Furthermore clear cyclic changes superimposed on the overall O−C diagram (particularly between −49000 to −32000 and also −15000 to 0 cycles) are observed. The further calculations of parameters listed in Table 4 all favor the presence of a magnetic cycle operating in this system.

Most of the published papers on contact binary systems (if not all), in recent years have discussed the operation of magnetic activity cycle in these systems (e.g. Maceroni & Van't Veer 1996; Quian et al. 2006, 2008; Bradstreet and Guinan 1994). As stated in the preceded subsection both of the components in EP And system can be magnetically active. Furthermore in Table 1 a large spotted area is reported.

Now it is a well-known fact that close binary systems with a cool F–K type star display enhanced magnetic activities. Short period close binaries (e.g., EP And) i.e., those having an orbital period $P < 5-6$ days, possess the above mentioned characteristics, due to rapid rotation (Richard & Albright 1993). Many authors (see e.g., Richards 1993, 1992; Hall 1989 & Olson 1981) have discussed that the secondary and/or primary in the close binaries having a late type component show a variety of time dependent magnetic properties, which may cause, brightness variations in the LC (particularly at mid primary eclipse), radiations of X-ray, Ultraviolet, infrared, and **cyclic variations in the orbital period of the binary** (through a mechanism purposed by Applegate 1992 and modified by Lanza et al. 1998 & Lanza 2005, 2006).

This mechanism is based on the variation of the active star shape through a change in the Gravitational Quadrupole Moment (GQM) of the star. This change in GQM is coupled to orbit, producing orbital period changes, which are briefly explained below: The GQM is the most sensitive to the rotation rate of the outer parts of the star. As the star goes through activity cycles, a magnetic torque is exerted on the outer parts of the star, the distribution of angular momentum changes resulting in a change in the oblatness of the star. These changes (of rotation rate and oblatness) will be communicated to the orbit by gravity, leading to orbital period variations. Lanza (2005; 2006) argued against this mechanism. Calculating the required power dissipated in one cycle theoretically, suggested an alternate modified model, emphasizing on the effects of intense magnetic fields, a fact which is possibly consistent with the rather high values of magnetic fields reported in the Table 4 of this work. Lanza found that surface angular velocity variation of secondary component required by Applegate's hypothesis is between 4–12 percent, i.e., too large to be compatible with observations and that kinetic energy dissipated in its convection zone ranges from 4–43 times that supplied by stellar luminosity along one cycle of the orbital period modulation. The estimated values of $\frac{\Delta\omega_1}{\omega_1} \simeq 0.0006, \frac{\Delta\omega_2}{\omega_2} \simeq 0.001$ in this work (Table 4) do support the results obtained by Lanza.

Finally, as stated earlier (in Section 5) the estimations of related stellar parameters (particularly ΔQ, the GQM) for EP And (Table 4) are in agreement with those estimated by Applegate (1992) and Lanza & Rodono (1999) for other similar systems, e.g., V 471 Tauri except **B** the magnetic field, which shows comparatively high values. These high values of **B** (while in rough agreement with Lanza's 2005 predictions), may also be attributed to the enhancement of fields, due to a rather low distance ($2.49R_{\odot}$) between the two components and interactions of the individual star B fields together, and also with the plasma ejected by the component stars. Though due to observed data deficiency all of the Applegate predictions (see Manzoori, 2009) can not be verified in this system, but according to the calculations performed in Section 5 (Table 4), the amplitude of angular velocity variations $\frac{\Delta\omega}{\omega} \sim 0.001$ is well-agreed with recent non-linear dynamo models (Covas, Moss & Tavakol 2005) for stars with deep convective envelope. Thus in the opinion of the author the 11.72 yr cycle obtained through Fourier analysis of P(E) function (see Section 4) is most likely due to magnetic cycle effect in this system.

6.6 Magnetic Braking

According to Bradstreet and Guinan (1994), Stepien (1995, 2006) the role of AML is crucial in the formation and evolution of the contact low mass binary stars. The magnetized star winds move outward from the active star, but are twisted due to rapid rotation of the star. Charged particles in the star wind get trapped in the magnetic field of the star and are dragged along the field lines. The result is AM transfer from the star by magnetic field to the charged particles. As the winds leave the star surface they are dragged by the magnetic field which, in turn, slows down rotation of the star. For close binaries in which synchronization of rotational and orbital period is expected, loss of rotational angular momentum occurs at the expense of orbital AM. As a result, the period decreases (consistent with the observations) i.e., the components spin up and approach one another to form a single rapid rotating star (see Stepien 1995; Skumanich

https://doi.org/10.1071/AS11003 Published online by Cambridge University Press

1972). As stated by Stepien (1995, 2006) contact binary stars are magnetically very active and it is generally accepted that they lose mass and AM via magnetized wind. Both components of the EP And system can be magnetically active, because the secondary is most likely a late type (as might be checked from the Figures 10–12), and the primary was also reported to be a F-type star (see Pribulla et al., 2001, also website `http://www.as.up.krakow.pl/o-c/data;`), moreover the assumed separation of the components is relatively low (2.49 $R_{\odot}$). Therefore, one expects the magnetic field interactions between the two components to be intensified and consequently its effect on the AML to be enhanced, due to formation of magnetic loops between the surface magnetic fields of the components (see also Uchida & Sakurai 1985). This statement is consistent with the Bradstreet and Guinan (1994) that the magnetic torque produced by magnetic field in the wind depends on the strength of magnetic field. But the details of this idea and its quantitive formulations and experimental verifications will remain a challenge for the future.

Finally by more careful inspections of the O–C curve (Figure 7) we can see two distinct parts of variations, first part from cycle −63720 (year 1931) to around −23970th cycle (year 1975) with a negative slope, and the second part from cycle −23970 (year 1975) onwards with a relatively smaller slope. The different slopes in two parts mentioned might be due to combination of three different effects namely, mass transfer, AML due to magnetic braking and presence of a third body. A third body when approaching the system would cause variations of O–C with relatively larger amplitude compared to the time of recedes, therefore the relatively larger slope of variation at first part may be related to period of approach and the second part to the receding interval.

6.7 Concluding Remark

Considering the above discussion and the results of LCs solutions obtained, we may conclude that the EP And is most probably a shallow over contact binary consisting of a normal Main Sequence star as primary and a relatively evolved MS as its secondary. The above mentioned cyclic period changes, together with the fact that the type of the component stars, are most probably later than F, which possess enhanced magnetic activities (due to existence of deep convective layers), led me to the conclusion that, apart from the mass transfer and light time effect, the most probable causes of period changes in this system are the magnetic activity cycle and magnetic braking through a mechanism described by Applegate (1992), modified by Lanza et al. (1998); Lanza & Rodono (1999, 2002) and Lanza (2005, 2006) on which the mass transfer effect is superimposed.

Acknowledgments

We acknowledge with thanks the variable star observations from the AAVSO International Database contributed by observers worldwide and used in this research. Also we have used data from the WASP public archive in this research. The WASP consortium comprises of the University of Cambridge, Keele University, University of Leicester, The Open University, The Queens University Belfast, St. Andrews University and the Isaac Newton Group. Funding for WASP comes from the consortium universities and from the UKs Science and Technology Facilities Council.

References

Applegate, J. H., 1992, ApJ, 385, 621
Biermann, P. & Hall, D. S., 1973, A&A, 27, 249
Binnendijk, L., VA, 1970, 217
Bradstree, D. H. & Guinan, E. F., 1994, Astronomical Society of the Pacific Conference series, 56, 228
Butters, et al., 2010, 520, L10
Covas, E., Moss, D. & Tavakol, R., 2005, A&A, 429, 657
D'Angelo, C., van Kerkwijk, M. H. & Rucinski, S., 2006, AJ, 132, 650
Filatov, G. S., 1960, ATsir, 215, 20
Flower, P. J., 1996, ApJ, 469, 355
Gazeas, K. & Stepien, K., 2008, MNRAS, 390, 1577
Gettel, S. J., Geske, M. T. & McKay, T. A., 2006, AJ, 131, 621
Glownia, Z., 2002, AdSpR, 6, 211
Hall, D. S., 1989, SSRV, 50, 219
Hilditch, R. W., 1989, SSRV, 50, 289
Huang, Su. Shu., 1963, ApJ, 138, 417
Huang, R. Q., Song, H. F. & Song, Lan Bi, S., 2007, ChJAA, 7, 235
Kalimeris, A., Livaniou, H. R. & Rovithis, P., 1994, A&A, 282, 775
Kaluzny, J. & Shara, M. M., 1987, ApJ, 314, 585
Kolopov, P. N., et al., 1985, General Catalogue of Variable Stars, Vol I (Moscow: Nauka)
Kuiper, G. P., 1941, APJ, 93, 133
Kwee, K. & Van Woerden, H. M., 1956, BAN, 12, 327
Lanza, A. F., 2005, MNRAS, 364, 238
Lanza, A. F., 2006, MNRAS, 369, 1773
Lanza, A. F. & Rodono, M., 2002, A&A, 390, 167
Lanza, A. F., Rodono, M. & Ronse, R., 1998, MNRAS, 296, 893
Lanza, A. F., Rodono, M. & Rosner, R., 1999, A&A, 296, 893
Li, L., Han, Z. & Zhang, F., 2004a, MNRAS, 351, 137
Li, L., Han, Z. & Zhang, F., 2004b, MNRAS, 355, 1383
Li, L., Han, Z. & Zhang, F., 2006, MNRAS, 360, 272
Lucy, L. B., 1968, APJ, 151, 1123
Lucy, L. B., 1976, APJ, 205, 482
Maceroni, C. & Van't, Veer, 1996, A&A, 311, 523
Manek, J., 1994, IBVS, 4116
Manzoori, D., 2007, PASA, 24, 1
Manzoori, D., 2008, APSS, 318, 57
Manzoori, D., 2009, AJ, 138, 1917
Olson, E. C., 1981, ApJ, 250, 704
Pribulla, T. & Rucinski, S. M., 2006, AJ, 131, 2986
Pribulla, T., Vanko, M. & Parimucha, S., 2001, IBVS, 5184
Prsa, A. & Zwitter, T., 2005, APJ, 628, 426
Prsa, A., Guinan, E. F., Devinney, E. J., De George, M., Bradstreet, D. H., Giammarco, J. M., Alcock, C. R. & Engle, S. G., 2008, APJ, 687, 542
Qian, S. & Ma, Y., 2001, PASP, 113, 754
Qian, S., Yang, Y., Zhu, L., He, J. & Yuang, J., 2006, ApSS, 304, 25
Qian, S., He, J. J. & Xiang, F. Y., 2008, PASJ, 60, 77
Richards, M. T., 1992, ApJ, 387, 329
Richards, M. T., 1993, ApJS, 86, 255
Richards, M. T. & Albright, G. E., 1993, ApJS, 88, 199
Rucinski, S. V., Pribulla, T. & van Kerkwijk, M. H., 2007, AJ, 134, 2353
Rucinski, S. V. & Duerbeck, H. W., 1997, PASP, 109, 1340
Siess, L., Dufour, E. & Forestini, M., 2000, A&A, 358, 593

https://doi.org/10.1071/AS11003 Published online by Cambridge University Press

Shu, F. H., Lubow, S. H. & Anderson, L., 1979, AJ, 209, 536
Skumanich, A., 1972, ApJ, 171, 565
Song, H. F., Huang, R. Q. & Bi, S. L., 2007, ChJAA, 7, 539
Stepien, K., 1995, MNRAS, 274, 1019
Stepien, K., 2006, AcA, 56, 347
Strohmeier, W., Geyer, E. & Kippenhahn, R., 1955, Kleine Veroff entlichugen der remis sternwate No. 11, Bamberg
Tokovinin, A., Thomas, S., Sterzik, M. & Udry, S., 2006, A&A, 450, 681
Tylenda, R., Hajduk, M., Kaminski, T., Udalski, A., Soszynski, I., Szymanski, M. K., Kubiak, M., Pietrzynski, G., Poleski, R., Wyrzykowski, L. & Ulaczyk, K., 2011, A&A, 528, 114
Uchida, Y. & Sakurai, T., 1985, IAUS, 107, 281
Van Hamme, W., 1993, AJ, 106, 2096
Van Hamme, W. & Wilson, R. E., 2003, ASP Conf. Ser. 298, GAIA
Wesselink, A. J., 1969, MNRAS, 144, 297
Wilson, R. E., Pettera, L. E. & Van Hamme, W., 1985, APJ, 289, 748
Wilson, R. E. & Caldwell, C. N., 1978, ApJ, 221, 917
Wilson, R. E. & Devinny, E. J., 1971, ApJ, 166, 605
Wilson, R. E. & Twigg, L. W., 1980, IAUS, 88, 263
Wilson, R. E. & Van Hamme, W., 2003, Computing Binary Star Observables (Gainsville, FL: Astronomy Dept., University of Florida)
Wilson, R. E., Van Hamme, W. & Pettera, L. A., 1985, APJ, 289, 748

https://doi.org/10.1071/AS11003 Published online by Cambridge University Press